RESEARCH ARTICLE

Ternary Solid Dispersion Improves Anti-cancer Activity of Alpha-mangostin Against MCF-7 Breast Cancer Cells

Arif Budiman[1,*], Ellen Nathania Yunita[1], Agus Rusdin[2], Jeremy Marcelino[1], Salma Amaliah[1], Diah Lia Aulifa[2]

[1]Departement of Pharmaceutics and Pharmaceutical Technology, Faculty of Pharmacy, Universitas Padjadjaran, Jl. Raya Bandung-Sumedang Km.21, Sumedang 45363, Indonesia
[2]Departement of Pharmaceutical Analysis and Medicinal Chemistry, Faculty of Pharmacy, Universitas Padjadjaran, Jl. Raya Bandung-Sumedang Km.21, Sumedang 45363, Indonesia

*Corresponding author. Email: arif.budiman@unpad.ac.id

Received date: Dec 6, 2025; Revised date: Feb 2, 2026; Accepted date: Feb 3, 2026

Abstract

BACKGROUND: Alpha-mangostin (AM) exhibits potent anti-breast cancer activity but its therapeutic effectiveness is constrained due to low aqueous solubility and poor bioavailability. Ternary solid dispersions (TSDs) were developed by adding another excipient to address these challenges. Nevertheless, limited studies have systematically evaluated whether improvements in dissolution and stability achieved through TSD systems are translated into enhanced *in vitro* cytotoxicity of AM. Therefore, TSD system of AM with Eudragit (EUD) and Poloxamer (POL) was developed, and *in vitro* cytotoxicity activity was evaluated as a preliminary proof-of-concept in MCF-7 breast cancer cells.

METHODS: TSD of AM was prepared by solvent evaporation and characterized by Power X-Ray Diffraction (PXRD), Differential Scanning Calorimetry (DSC), and Fourier Transform Infrared (FT-IR) Spectroscopy. The pharmaceutical properties were evaluated by *in vitro* dissolution test using a standard paddle apparatus, while physical stability was assessed under two relative humidity environments. The *in vitro* anticancer efficacy was examined in MCF-7 breast cancer cell using an MTT assay.

RESULTS: Amorphization of TSD was confirmed by a halo pattern with PXRD measurements and the absence of an AM melting peak in the DSC curve. FT-IR analysis revealed hydrogen bond interactions between the carbonyl group of AM and EUD/POL protons. TSD system significantly improved the dissolution profile and enhanced cytotoxic effects, reducing cell viability to 1.17% at 16 µg/mL with an IC_{50} of 7.11 µg/mL (CI 95%: 6.626-7.591).

CONCLUSION: The TSD system significantly improved dissolution profile and *in vitro* cytotoxicity in MCF-7 breast cancer cells, providing proof-of-concept for enhancing the biological performance of AM.

KEYWORDS: alpha-mangostin, ternary solid dispersions, dissolution, MCF-7, cytotoxicity

Indones Biomed J. 2026; 18(1): 77-87

Introduction

Cancer remains one of the leading causes of morbidity and mortality worldwide, with current therapies often limited by drug resistance, systemic toxicity, and suboptimal efficacy. (1) Breast cancer, a heterogeneous disease encompassing distinct molecular and epidemiological subtypes, is the most prevalent malignancy among women and a major contributor of cancer-related deaths globally.(2,3) Breast cancer represents nearly one-third of all cancers diagnosed in women, and roughly 15% of those diagnosed eventually result in mortality.(4–6) Although countries with higher income levels tend to show greater incidence, the burden of death is more pronounced in low- and middle-income regions, largely because screening and advanced therapeutic

options are less accessible.(5) Despite therapeutic advances, the growing global burden underscores the need for more effective and accessible therapeutic strategies, including the development of potent agents derived from natural sources.(7)

Alpha-mangostin (AM), a major xanthone derivative from mangosteen peel, exhibits potent anti-breast cancer activity by inhibiting proliferation and inducing apoptosis in MCF-7 and T47D cells through fatty acid synthase (FAS) inhibition and modulation of the human epidermal growth factor receptor 2 (HER2)/phosphoinositide 3-kinase (PI3K)/protein kinase B (Akt) and mitogen-activated protein kinase (MAPK) pathways.(8–10) However, its clinical potential is constrained by extremely low aqueous solubility and poor bioavailability, leading to limited therapeutic efficacy.

Amorphization enhances the solubility and dissolution of poorly water-soluble drugs by disrupting the crystalline lattice and increasing molecular mobility in solution. However, amorphous drugs are thermodynamically unstable and prone to recrystallization. Amorphous solid dispersion (ASD) systems stabilize amorphous drugs by dispersing them within a polymer matrix, where strong interactions, such as hydrogen bonding, suppress recrystallization and enhance dissolution.(11–13) Despite this effectiveness, some ASD remains limited by poor wettability and physical instability, which may restrict drug release and formulation performance.(14) To overcome these limitations, ternary solid dispersions (TSDs) have been developed by incorporating an additional excipient to further refine the physicochemical characteristics of the systems.(15)

In a TSD system, the active substance is homogenously dispersed within two distinct carriers in solid form, where the presence of the third component improves wettability, solubility, stability, and reinforcing molecular interactions, thereby minimizing recrystallization risk.(16) Moreover, TSDs have been shown to enhance drug release, bioavailability, and pharmacological efficacy, as the synergistic effect of the added excipient facilitates more efficient drug delivery.(17–19) This approach is particularly advantageous for poorly soluble drugs that require advanced formulation strategies to achieve optimal dissolution and therapeutic activity.

Our previous studies on binary AM–Eudragit (EUD) ASDs demonstrated improved solubility compared to crystalline AM; however, drug release remained suboptimal due to poor wettability and agglomeration in the dissolution medium.(20) Therefore, this study aims to develop a TSD system of AM with EUD and POL and evaluate this impact on solubility, dissolution, stability, as well as anticancer efficacy against breast cancer cells. POL was selected as a third component because it is commonly used in TSD systems to enhance drug solubility, wettability, and stability, thereby improving dissolution performance.(21,22) Furthermore, previous research has indicated that the addition of POL (188/407), particularly in dexibuprofen formulations with hydroxypropyl-β-cyclodextrin (HPβCD), markedly enhanced solubility, stability, and drug release rate.(22)

Methods

Preparation of TSDs

AM with a molecular weight of 410.5 g/mol (Chengdu Biopurify Phytochemicals, Shincuan, China), Eudragit L100 (JJ Degussa Chem, Bangkok, Thailand) and poloxamer 407 (Sigma-Aldrich, St. Louis, MO, USA) were bought and prepared. A TSD of AM was prepared via the solvent evaporation method. AM with EUD and POL at molar ratios of 1:4:1, 1:4:3, and 1:4:5 was dissolved in methanol. The solvent was evaporated with a rotary evaporator (Rotavapor, Buchi EL 13; Buchi, Flawil, Switzerland), set at a water bath of 40°C. The residual solvent was entirely eliminated by oven drying at 40°C for 72 h to yield the samples. Chemical structure of AM, Eudragit L100, and poloxamer 407 were illustrated in Figure 1.

Powder X-Ray Diffraction (PXRD) Measurement

PXRD patterns were acquired utilizing a Kristalloflex diffractometer (Bruker D8 Advance; Siemens, Berlin,

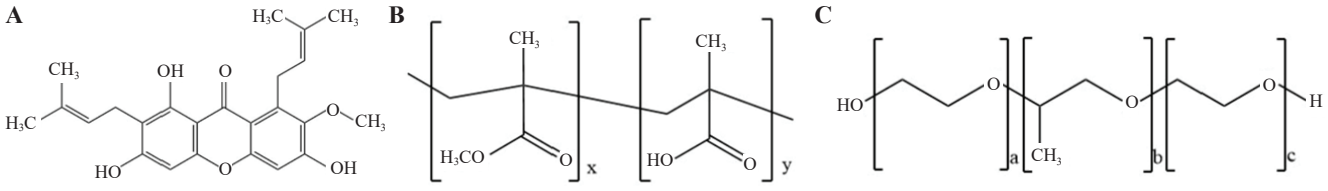

Figure 1. Structure of the materials used. A: Alpha-mangostin. B: Eudragit L100. C: Poloxamer 407.

Germany). The instrument operated with Cu target to generate Kα radiation, maintained at a voltage of 40 kV and a current of 40 mA. Data collection covered a diffraction angle range of 3° to 40° (2θ).

Differential Scanning Calorimetry (DSC) Measurement

DSC thermograms were generated using Shimadzu DSC-60 Plus system (Shimadzu, Kyoto, Japan). Samples weighing approximately 3-5 mg were encapsulated in crimped aluminum pans and subjected to a continuous nitrogen purge at 20 mL/min. Thermal scanning was conducted over a temperature range of 0°C to 250°C, employing a linear heating rate of 10°C/min.

Fourier Transform Infrared (FT-IR) Spectroscopy

FT-IR spectroscopy was employed to investigate potential intermolecular interactions between the active substance and the polymer carrier, utilizing a Prestige21 system (Shimadzu). Sample preparation followed the conventional KBr pelleting protocol; approximately 1-2 mg of isolate was finely ground with 200-250 mg of potassium bromide to ensure uniform dispersion. The resulting powder blend was compressed at 6- Psi into discs, and spectral analysis was conducted within the 4000-400 cm^{-1}.

Entrapment Efficiency Test

Drug entrapment efficiency for the various TSD ratios was determined by preparing methanolic solutions with a theoretical drug concentration of 100 µg/mL. The preparations were stirred for 30 minutes to facilitate extraction, followed by filtration through a 0.45 µm membrane. The resulting filtrate was then diluted with acetonitrile and subjected to HPLC analysis to quantify the entrapped drug.

$$\% \text{ Entrapment efficiency} = \frac{\text{Measured concentration}}{\text{Theoritical concentration}} \times 100\%$$

High Performance Liquid Chromatography (HPLC) Conditions

HPLC analysis was carried out using a Dionex Ultimate 3000 HPLC (Dionex, Sunnyvale, CA, USA). Sample was injected into an Inertsil ODS C18 (GL Science, Torrance, California, USA) with a 4.6×150 mm column at 30°C, while the composition of the mobile phase was acetonitrile and 0.1% formic acid in water at a ratio of 95:5. The samples were detected using a UV detector at a wavelength of 244 nm, and the standard solutions were prepared in the mobile phase with concentrations of 5, 10, 50, 100, and 200 µg/mL.

Crystalline and Amorphous Solubility Determination

Equilibrium solubility determinations for both crystalline AM and the solvent-evaporated TSD were carried out by introducing an excess amount of the solid material into 50 mM phosphate buffer (pH 7.4). These suspensions were maintained at 37°C under continuous agitation for a 48-hour period to facilitate saturation. Following this equilibration phase, the supernatants were clarified using a 0.45 µm membrane filter, diluted with the chromatographic mobile phase, and the dissolved drug concentration was subsequently quantified via HPLC.

Dissolution Experiment

In vitro release kinetics were investigated using a standard paddle apparatus setup. The dissolution medium consisted of 500 mL of 50 mM phosphate buffer (pH 7.4) maintained at 37°C, with powder samples dispersed to achieve a theoretical concentration of 50 µg/mL under constant agitation at 150 rpm. Sample aliquots (5 mL) were collected at specific intervals across a 2-hour duration (5, 10, 20, 30, 45, 60, 90, and 120 minutes). Prior to HPLC quantification, the withdrawn fluids were clarified through a 0.45 µm membrane filter and subsequently diluted with acetonitrile.

Storage Stability Study

Physical stability was evaluated by subjecting samples to two distinct relative humidity (RH) environments within controlled desiccators at 25°C: a) dry conditions (0% RH) maintained by silica gel, and b) high humidity (90% RH) generated by a saturated potassium nitrate solution. Solid-state phase transformations were subsequently monitored via PXRD at predetermined intervals 0, 4, 19, 30, and 37 days.(23)

Cytotoxic Study on MCF-7 Breast Cancer Cell Line

The anticancer efficacy of AM and its TSD formulations was evaluated using MCF-7 breast cancer cell lines. MCF-7 (American Type Culture Collection/ATCC, Manassas, VA, USA) were cultured in Roswell Park Memorial Institute (RPMI) medium supplemented with 10% (v/v) fetal bovine serum (FBS) and 1% penicillin-streptomycin, and maintained at 37°C in a humidified incubator with 5% CO_2. Cells were routinely tested for mycoplasma contamination and used within a limited number of passages to ensure cell line authenticity. For cytotoxicity evaluation, cells were seeded into 96-well plates at a density of 1×10^4 cells per well in 200 µL of complete culture medium and incubated for 24 h to allow cell attachment, reaching approximately 80% confluency. Pure AM, binary ASD, and TSD-AM

were prepared by dissolving samples in dimethyl sulfoxide (DMSO), followed by serial dilution with RPMI medium to obtain final concentrations of 0, 4, 6, 8, 10, 12, 14, and 16 µg/mL, with the final DMSO concentration maintained below 0.5% (v/v). All treatment concentrations were expressed as AM-equivalent concentrations (µg/mL), calculated based on the AM content (10% and 20% w/w) in each formulation. Based on the highest AM-equivalent treatment concentration and the formula composition, the corresponding maximum calculated concentrations of EUD and POL were 10.8 µg/mL and 8.1 µg/mL, respectively. Cells were treated with the formulations and incubated for 48 h under the same culture conditions. After incubation, the cells were washed twice with PBS. The 0.5 mg/mL of MTT solution (Sigma-Aldrich) was added to each well and the plates were incubated for 2–4 hours at 37°C to allow the formation of formazan crystals. Subsequently, 100 µL sodium dodecyl sulfate (SDS) in 0.01 N HCl was added to each well as a stopping solution. Plates were covered with foil and incubated overnight at room temperature. Cell viability was determined using a microplate reader at 550 nm. All experiments were performed in triplicate as technical replicates.

Statistical Analysis

The data were analyzed using GraphPad Prism 10.6.1 (GraphPad Software, Boston, MA, USA). Statistical analyses were performed using one-way ANOVA followed by Tukey's multiple comparison. The statistical significance was set at 95% confidence level and indicated by *p*-values, with asterisks denoting the levels of significance (*$p<0.05$, **$p<0.01$).

Results

Characterization Study Results

Based on the XRD diffractogram results obtained in Figure 2A, AM crystal and AM prepared by solvent evaporation (AM SE) showed characteristic diffraction peaks, indicating that amorphous AM was not formed due to its high recrystallization tendency. Meanwhile, the TSD AM with ratios of 1:4:1, 1:4:3, and 1:4:5 showed a halo pattern without characteristic diffraction peaks, suggesting the formation of an amorphous form.

The DSC profile of AM and AM SE showed an endothermic melting peak at around 177°C as shown in Figure 2B, indicating the melting point of the compound. Meanwhile, in the thermogram of the TSD AM with ratios of 1:4:1, 1:4:3, and 1:4:5, no endothermic melting peak of AM was found. This indicated that the AM has transformed from a crystalline form into an amorphous form. The amount of polymers in the form of EUD and POL was sufficient to stabilize all AM in amorphous form even at a ratio of 1:4:1. FT-IR spectroscopy was used to determine the interaction between the drug and the polymer in the TSD system of AM. Figure 2C showed the spectrum of AM at wave numbers 3417, 2930, 1617, 1461, and 1288 cm^{-1}, which represent the OH stretching, C-H, C=O, C=C, and C-O functional groups, respectively. TSD AM with various compositions showed shifts in functional groups on the FT-IR spectrum. In the TSD spectrum of AM with a ratio of 1:4:1, there was a shift in the OH group to 3450 and 3233 cm^{-1}; the CH group to 2612 and 2939 cm^{-1}; the C=O group to 1613; the C=C group shifts to 1612 cm_{-1}; the C-O group shifts to 1170 cm^{-1}.

In the TSD spectrum of AM with a ratio of 1:4:3, there was a shift of the OH group to 3438 cm^{-1}; the CH group to 2931 and 2607 cm^{-1}; the C=O group to 1624; the C=C group shifted to 1370 cm^{-1}; the C-O group shifts to 1173 cm^{-1}. There was a shift in the OH group of EUD from 3200 to 3450 and 3438 cm^{-1}, respectively, at TSD AM 1:4:1 and 1:4:3. This shift had a different wavelength compared to the SD AM-EUD 1:4 form, which had a value of 3590 cm^{-1}. This indicates that in the TSD system, there is interaction not only with EUD but also with POL. In the SD AM-EUD 1:4 system, there was no shift in the carbonyl group, but in the TSD system, both ratios showed a shift from 1642 to 1718 cm^{-1}.

The TSD systems of AM with EUD and POL at ratios of 1:4:1 and 1:4:3 achieved 100% entrapment efficiency. This result confirmed the effective entrapment of AM within the EUD–POL matrix, indicating strong drug–polymer–polymer interaction, respectively, resulting in a high concentration in the TSD system.

The equilibrium solubility of AM was evaluated in 50 mM phosphate buffer (pH 7.4) at 37°C. The crystalline form of AM exhibited a solubility of 0.43±0.30 µg/mL, confirming its extremely poor aqueous solubility. The amorphous form showed only a slight improvement, reaching 0.44±0.06 µg/mL (1.02-fold) due to high recrystallization tendency. The binary ASD of AM using EUD markedly enhanced solubility to 15.24±2.17 µg/mL, representing approximately a 35.44-fold increase compared to crystalline AM. A further significant enhancement was achieved by adding POL as the third component. The TSD systems with ratios of 1:4:1 and 1:4:3 exhibited solubility values of 40.53±1.26 µg/mL and 46.28±0.38 µg/mL, corresponding to 90.54- and 107.63-fold increases, respectively. These results indicated that the

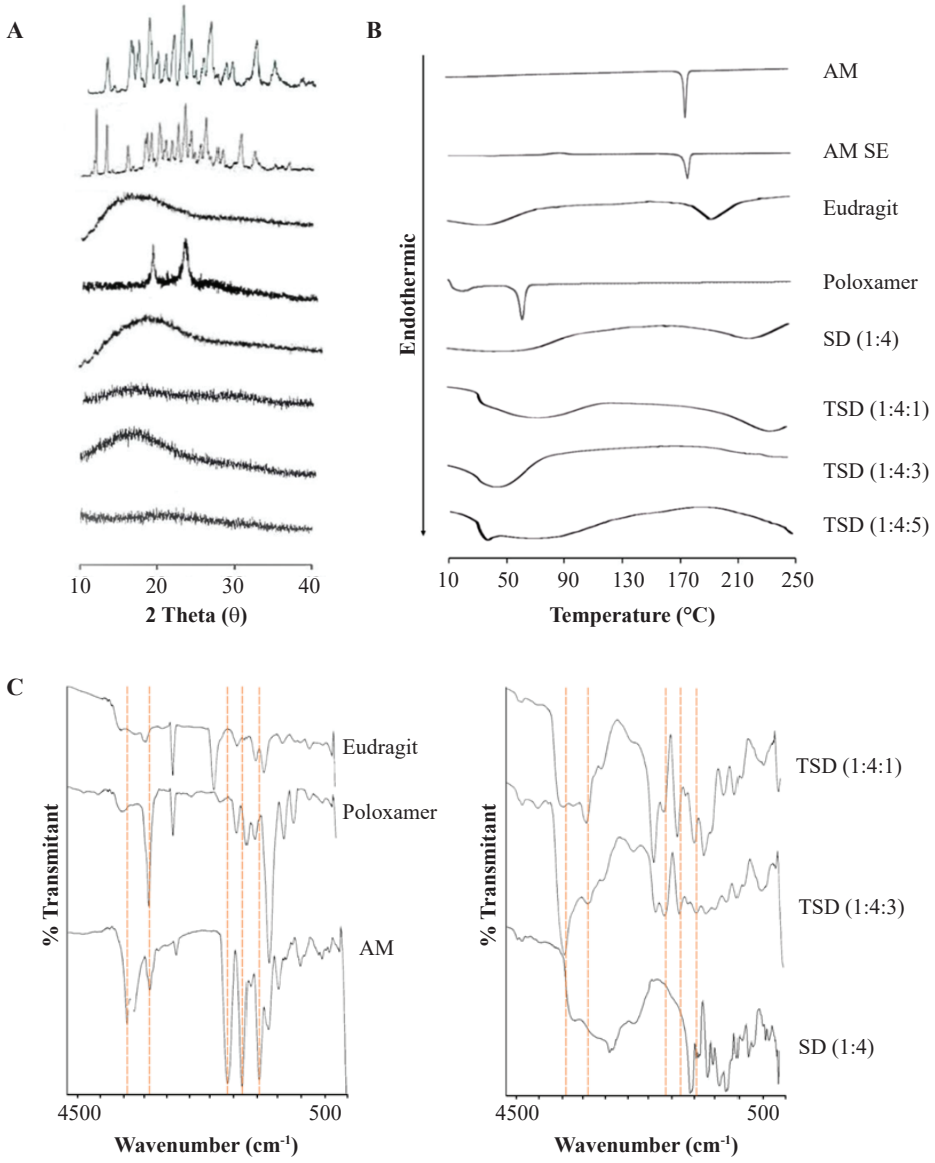

Figure 2. Characterization of TSD AM. A: Powder X-Ray Diffraction (PXRD) Patterns. B: Differential Scanning Calorimetry (DSC) Curves. C: FT-IR Spectra. The PXRD diffractogram exhibited a halo pattern, whereas the DSC thermogram indicated the absence of the AM melting point, suggesting the successful amorphization of the TSD formulation. The spectroscopic data indicated a peak shift, suggesting an interaction between the active substance and the polymer.

combination of EUD and POL in a TSD system effectively enhances the solubility of AM compared to crystalline and binary ASD.

TSD Pharmaceutical Properties Results

The dissolution profile of crystalline AM exhibited a slow dissolution rate, reaching a maximum concentration of only 0.18 µg/mL. In contrast, both TSD formulations with ratios of 1:4:1 and 1:4:3 showed markedly improved dissolution compared to the binary ASD (1:4) (Figure 3). The TSD 1:4:3 formulation achieved the highest drug release, reaching approximately 50 µg/mL. The enhanced dissolution is attributed to improved wettability from the addition of POL, which increased surface area and promoted better drug dispersion. Moreover, no decline in AM concentration was observed, indicating that the TSD maintained the amorphous state and prevented recrystallization in the aqueous medium.

The physical stability test of the TSD of AM under 0% and 90% RH conditions demonstrated excellent stability. No evidence of recrystallization was observed up to day 30 at 0% RH and up to day 37 at 90% RH. The diffractogram of TSD AM (Figure 4) exhibited a characteristic halo pattern without distinct diffraction peaks, confirming its amorphous nature. These findings indicated that the addition of polymers within the TSD matrix effectively preserved the amorphous state of AM and prevented recrystallization during storage.

Cytotoxic Profile of TSD-AM on MCF-7 Breast Cancer Cell Line

The cytotoxicity evaluation demonstrated significant differences in % cell viability among the tested formulations, highlighting the enhanced anticancer potential of TSD systems compared to binary and pure AM in PBS (Figure

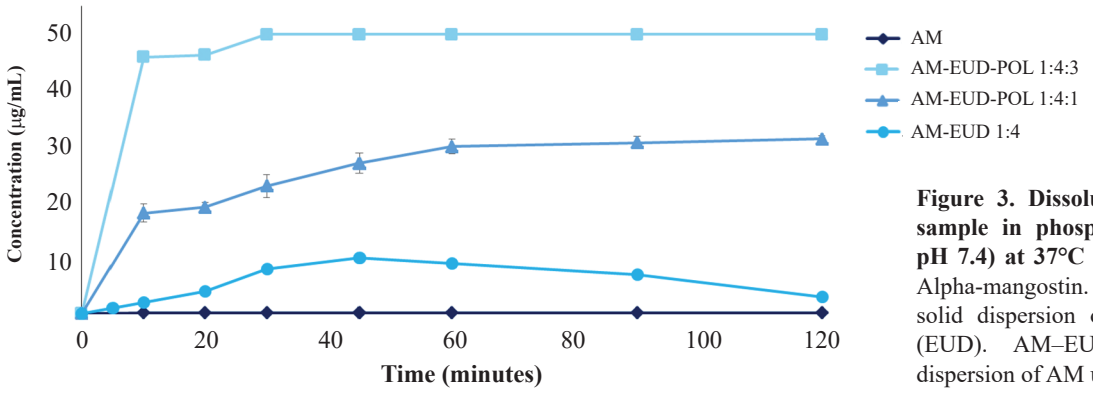

Figure 3. Dissolution profiles of each sample in phosphate buffer (50 mM, pH 7.4) at 37°C (n=3, mean±SD). AM: Alpha-mangostin. AM–EUD: Amorphous solid dispersion of AM using Eudragit (EUD). AM–EUD–POL: Ternary solid dispersion of AM using EUD and POL.

5A). Pure AM in PBS exhibited minimal cytotoxic activity, with % cell viability consistently above 85% across all concentrations, even reaching 85.88% at 16 µg/mL. This low cytotoxicity is likely due to the poor aqueous solubility of AM in its crystalline form, which limits its bioavailability and ability to exert therapeutic effects on cancer cells.

In contrast, the binary ASD systems (AM–EUD) displayed marked reductions in cell viability, particularly at higher concentrations. At 16 µg/mL, AM–EUD showed % cell viability of 4.12%. This suggested that the use of polymers, particularly EUD in AM–EUD, significantly enhances the solubility and bioavailability of AM, leading to improved cellular uptake and increased cytotoxic effects. The higher efficacy of AM–EUD may be attributed to the polymer's ability to provide sustained release, improve drug wettability, and inhibit recrystallization, thereby increasing the availability of AM in its amorphous state to interact with cancer cells.

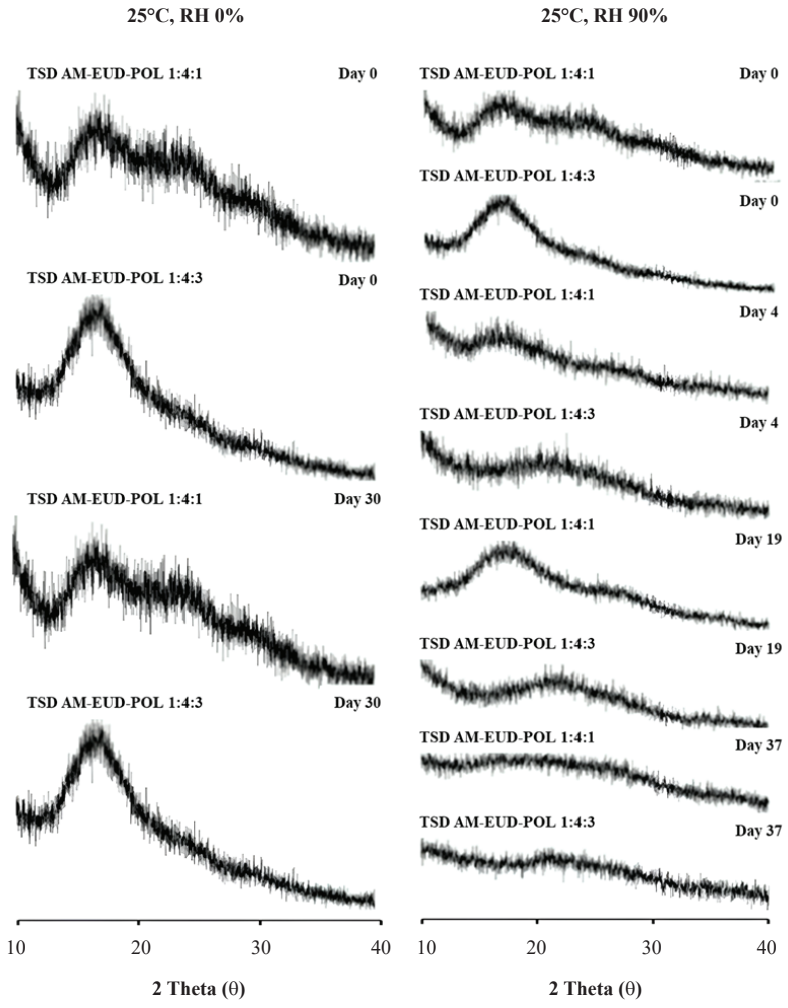

Figure 4. PXRD patterns of TSD AM (ratios 1:4:1 and 1:4:3) after storage at 25°C under different RH conditions (0% and 90%). The X-axis represents the diffraction angle (2θ, degrees). Diffractograms collected up to Day 30 (0% RH) and Day 37 (90% RH) displayed halo patterns with no crystalline peaks, indicating the absence of recrystallization and confirming the excellent physical stability of the TSD systems.

The TSD systems (AM–EUD–POL) further amplified the cytotoxic effects. Notably, AM–EUD–POL achieved the lowest % cell viability, reducing it to 1.17% at 16 µg/mL. The exceptional efficacy of AM–EUD–POL can be attributed to several synergistic effects introduced by the combination of EUD and POL. EUD provides a stable protective matrix, which not only prevents the recrystallization of AM but also ensures prolonged retention and controlled release of the drug. POL, with its amphiphilic properties, enhances wettability by forming micelles, which facilitate better dispersion of AM in aqueous environments. Additionally, POL contributes to improved surface activity, reducing interfacial tension between the drug particles and the dissolution medium, further accelerating solubilization and cellular uptake. These combined effects enable a more efficient delivery of AM to the cancer cells, enhancing its cytotoxic potential.

The IC_{50} values of AM-EUD and AM-EUD-POL were determined with 95% confidence intervals: 7.31 µg/mL (CI: 5.955-8.599) and 6.74 µg/mL (CI: 6.012-7.447), respectively. Although AM-EUD-POL exhibited a numerically lower IC50 value, no statistically significant difference was observed between the two formulations (Figure 5B). Despite the absence of a statistically significant difference, AM-EUD-POL showed a tendency toward a lower IC50 value compared to AM-EUD, which may indicate a potential enhancement in cytotoxic response.

Discussion

In this study, AM was selected as the API and formulated a binary AM-EUD system and ternary AM-EUD-POL. The optimized formulation successfully incorporated the drug into the polymer matrix, as indicated by the physicochemical characterization. Crystalline AM exhibited poor solubility and slow dissolution, resulting in low drug concentration in the medium and minimal cytotoxicity. The amorphous form of AM without polymer showed slightly improved solubility compared to the crystalline form; however, its high recrystallization tendency led to rapid conversion to the crystalline state during dissolution, thereby reducing supersaturation and limiting drug release.(24) The binary AM–EUD system demonstrated greater solubility than pure AM; however, incomplete wetting and particle agglomeration continued to hinder drug release. This can be explained by the partial recrystallization of AM in the bulk medium, while the remaining portion dissolved gradually over time. Similar observations were reported in previous studies, where drug particle aggregation reduced the effective surface area, consequently decreasing wettability, and slowing dissolution.(25,26) The addition of POL into the AM-EUD to form a TSD system markedly enhanced solubility, dissolution rate, and physical stability, as evidenced by the absence of recrystallization during storage. These improvements are likely due to strong intermolecular interactions among AM, EUD, and POL that stabilize the amorphous structure and maintain a supersaturated state. Comparable findings have been reported in other TSD systems, where the addition of polymers such as POL improved wettability, dispersion uniformity, and crystallization inhibition through synergistic drug–polymer–polymer interactions.(21,22)

The enhanced physicochemical properties of AM were directly reflected in improved *in vitro* cytotoxic performance. The AM-EUD and AM-EUD-POL systems

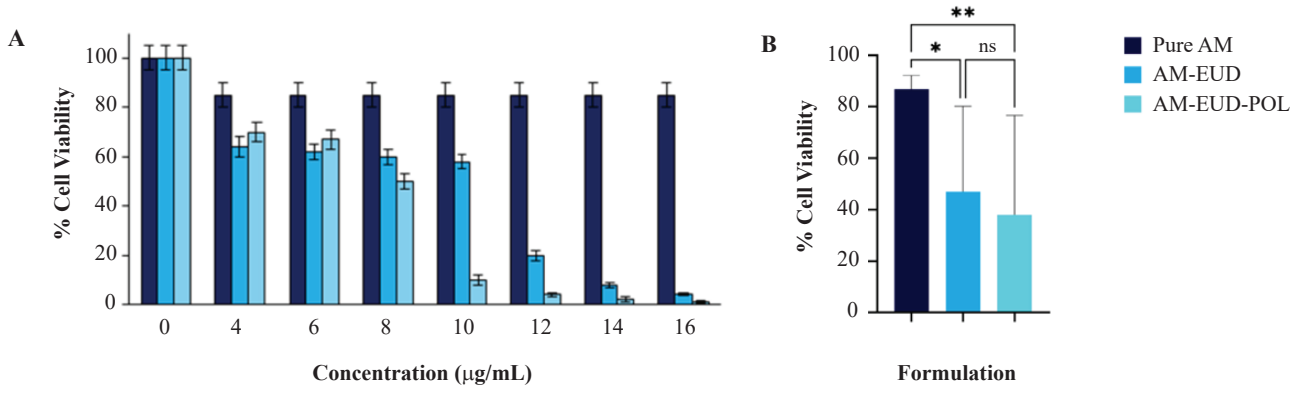

Figure 5. Cytotoxic evaluation of AM formulations. A: Concentration-dependent cytotoxic effects. B: Statistical comparison of cell viability between groups. Data are presented as mean±SD (n=3). Asterisks denote significant differences (*p<0.05, **p<0.01), while 'ns' indicates a non-significant difference. AM: Alpha-mangostin. AM–EUD: Amorphous solid dispersion of AM using Eudragit (EUD). AM–EUD–POL: Ternary solid dispersion of AM using EUD and POL.

showed lower cell viability than pure AM. Although AM-EUD-POL exhibited a numerical lower IC_{50} value, no statistically significant difference was observed between the AM-EUD-POL and AM-EUD formulations. Therefore, any potential enhancement in cytotoxic response should be interpreted with caution and requires further confirmation. In line with this observation, previous studies have reported variable cytotoxic effects on MCF-7 cells, highlighting the necessity for formulation techniques such as TSD to augment efficacy.(27) The increased cytotoxicity observed in TSD systems can be attributed to the enhanced dissolution rate and apparent solubility of AM, which facilitates drug diffusion and intracellular accumulation. The amorphous state promotes molecular dispersion, enabling efficient membrane permeation and stronger interactions with intracellular targets.(28,29) Efficient permeation is crucial, as it may facilitate intracellular exposure and could potentially contribute to apoptosis-related effects reported in previous studies (30), although such effects cannot be concluded from MTT data alone. Sustained supersaturation further ensures prolonged drug exposure to cancer cells, thereby strengthening the inhibition of cell proliferation. (31) The enhanced cytotoxic observed may be associated with apoptotic-related pathways, as suggested by previous studies, although this mechanism was not directly investigated in the present work. Previous studies have reported that AM can modulate apoptosis-related pathways, including FAS and HER2/PI3K/Akt and MAPK signaling. (32) In the present study, such mechanisms are proposed as hypotheses that may be associated with the observed cytotoxicity but were not experimentally validated. These findings highlight the potential of the TSD system as an effective formulation strategy for improving the anticancer delivery of poorly soluble drugs.(31,33,34)

From a formulation standpoint, the final excipient concentrations corresponding to the TSD formulation ratio (1:4:3) were calculated. The maximum concentrations of EUD and POL reached were 10.8 µg/mL and 8.1 µg/mL, respectively. A limitation of this study is that blank polymer controls were not included; therefore, excipient-related effects cannot be completely ruled out. Nevertheless, these final concentrations are substantially lower than commonly reported in polymer-based anticancer delivery systems, in which EUD has been evaluated *in vitro* at concentration up to 50 µg/mL, while POL has been employed as a delivery matrix at a concentration of 25% (w/v). Accordingly, the contribution of excipients to the observed cytotoxic effects is likely limited, and the biological responses observed in this

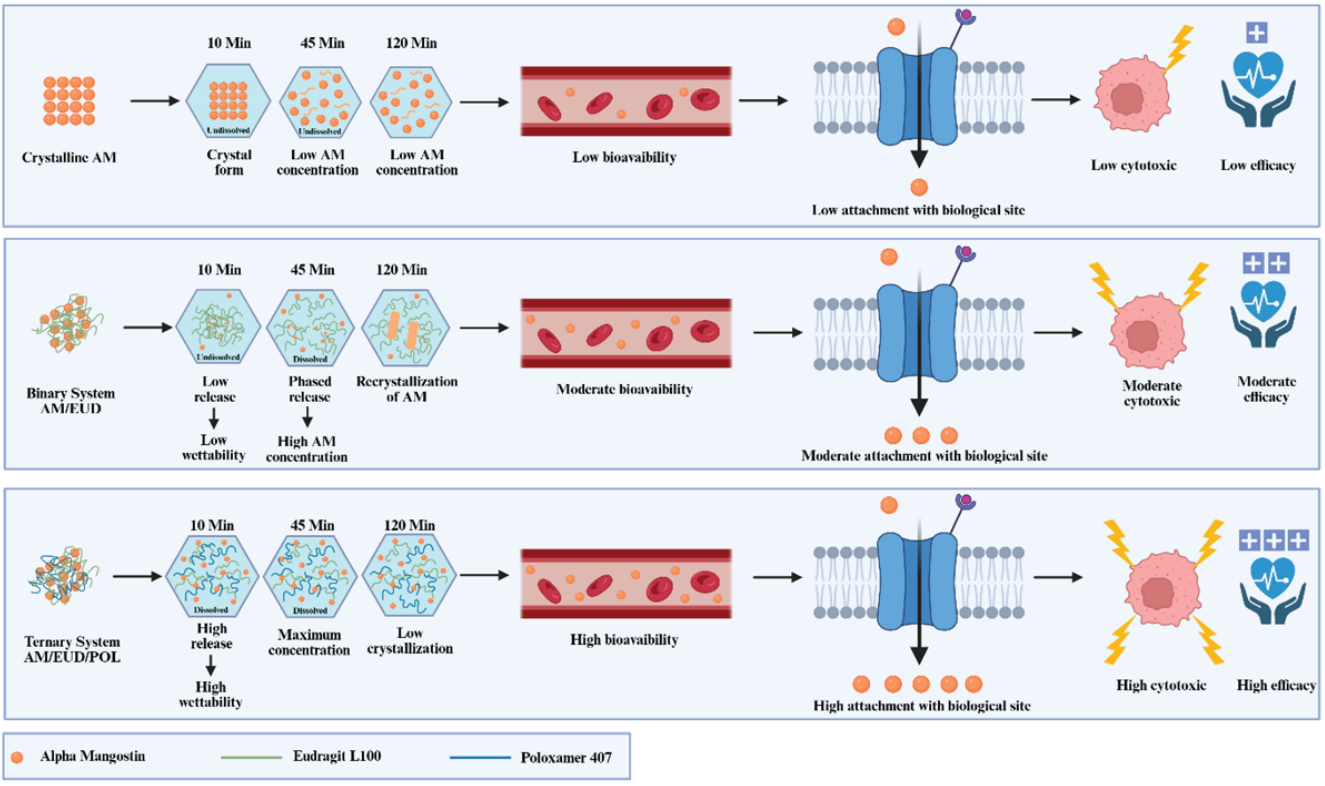

Figure 6. Schematic illustration of the proposed (hypothetical) mechanism underlying the improved *in vitro* cytotoxicity of AM in the TSD system.

study are predominantly attribute to the active compound rather than the carrier system.(35,36)

The speculated mechanism underlying the improved *in vitro* cytotoxicity of AM in the TSD system is illustrated in Figure 6. Mechanistically, the performance of the TSD systems results from its ability to stabilize the amorphous form of AM while leveraging the complementary functions of both polymers. EUD enhances solubility and inhibits recrystallization through hydrogen bonding (20,26,37), whereas POL, as a secondary polymer, introduces additive and synergistic effects such as stronger hydrogen bonding, improved wettability, higher surface activity, and finer drug dispersion. In particular, POL contributes to particle stabilization and enhances the solubility of the active substance by preventing particle aggregation and improving the contact between AM and the dissolution medium.(22,38) These factors lead to higher drug concentrations at the cellular interface and stronger cytotoxic effects compared to binary systems and pure AM.

Collectively, the cytotoxicity results provide preliminary proof-of-concept evidence supporting the potential of TSD-based formulations to enhance *in vitro* cytotoxicity through improved dissolution and availability. The combination of polymers plays a pivotal role in optimizing drug delivery and therapeutic performance. By maintaining amorphous stability, improving wettability, solubility, and dissolution, and enhancing cellular uptake, the TSD approach represents a promising formulation strategy for enhancing *in vitro* performance of poorly soluble drugs. These results provide a solid basis for further exploration of TSD systems in pharmaceutical and biomedical research, particularly anticancer therapy.

This study demonstrates clear advantages of the TSD AM system. However, several limitations should be acknowledged. The anticancer evaluation was restricted to *in vitro* cytotoxicity assays, which may not fully represent the complexity of *in vivo* tumor physiology, including drug metabolism, biodistribution, and interactions within the tumor microenvironment. The proposed mechanisms, particularly those related to apoptosis, were inferred rather than confirmed through molecular assays. In addition, only two polymer ratios were examined, thereby narrowing the scope of formulation optimization. Future research should incorporate *in vivo* pharmacokinetic and anticancer studies, molecular confirmation of apoptosis-related mechanisms, long-term stability testing under stress conditions, and expanded formulation design, including alternative third components or scalable manufacturing approaches, to support the progression of this TSD system toward preclinical and clinical development.

Conclusion

This study demonstrates that the formulation of AM within the TSD system provides preliminary proof-of-concept evidence for enhancing its *in vitro* cytotoxicity against MCF-7 breast cancer cells. The improved biological performance is consistent with enhanced pharmaceutical properties, particularly the stabilization of the amorphous form and improved dissolution behavior. Hence, these findings support the potential of TSD-based formulations as a promising strategy for improving the *in vitro* performance of poorly soluble anticancer compounds.

Acknowledgments

We would like to thank the Prodia Education and Research Institute (PERI) for supporting this work. This research was funded by PERI's Research Grant 2024 awarded to Arif Budiman (No. 031/RC/ResGrant/RD/2025/PERI; No. 251/UN6.O/HK.07.00/2025-PKS).

Authors Contribution

AB and DLA were involved in concepting and planning the research. ENY, AR, and SA performed the data acquisition/collection. ENY and AR calculated the experimental data and performed the analysis. AB, JM, and SA drafted the manuscript and designed the figures. DLA aided in interpreting the results. AB also secured the research funding. All authors took part in giving critical revision of the manuscript.

Conflict of Interest

The authors declare no conflicts of interest or competing interests related to the content of this manuscript.

References

1. Zafar A, Khatoon S, Khan MJ, Abu J, Naeem A. Advancements and limitations in traditional anti-cancer therapies: a comprehensive review of surgery, chemotherapy, radiation therapy, and hormonal therapy. Discov Oncol. 2025; 16(1): 607. doi: 10.1007/s12672-025-02198-8.
2. Abdihalim TS, Idris AAA. Mucin level as a potential biomarker for breast cancer diagnosis. Mol Cell Biomed Sci. 2022; 6(3): 117–20.

3. Prayogo AA, Wijaya AY, Hendrata WM, Looi SS, I'tishom R, Hakim L, *et al.* Dedifferentiation of MCF-7 breast cancer continuous cell line, development of breast cancer stem cells (BCSCs) enriched culture and biomarker analysis. Indones Biomed J. 2020; 12(2): 115–23.
4. Xu Y, Gong M, Wang Y, Yang Y, Liu S, Zeng Q. Global trends and forecasts of breast cancer incidence and deaths. Sci Data. 2023; 10(1): 334. doi: 10.1038/s41597-023-02253-5.
5. Siegel Mph RL, Giaquinto AN, Ahmedin |, Dvm J, Siegel RL. Cancer statistics, 2024. CA Cancer J Clin. 2024; 74(1): 12–49.
6. Wu J, Fan D, Shao Z, Xu B, Ren G, Jiang Z, *et al.* CACA Guidelines for Holistic Integrative Management of Breast Cancer. Holist Integr Oncol. 2022; 1(1): 7. doi: 10.1007/s44178-022-00007-8.
7. Rahmawati DR, Murwanti R, Jenie RI, Nurrochmad A. Pentagamavunon-1 enhances the anticancer effects of doxorubicin on triple-negative breast cancer cells in monolayers and 3D cancer spheroid models. Indones Biomed J. 2025; 17(3): 241–51.
8. Kurose H, Shibata MA, Iinuma M, Otsuki Y. Alterations in cell cycle and induction of apoptotic cell death in breast cancer cells treated with α-mangostin extracted from mangosteen pericarp. Biomed Res Int. 2012; 2012(1): 672428. doi: 10.1155/2012/672428.
9. Setiawati A. Anticancer activity of mangosteen pericarp dry extract against MCF-7 breast cancer cell line through estrogen receptor-A. Indones J Pharm. 2014; 25(3): 119–24.
10. Kritsanawong S, Innajak S, Imoto M, Watanapokasin R. Antiproliferative and apoptosis induction of α-mangostin in T47D breast cancer cells. Int J Oncol. 2016; 48(5): 2155–65.
11. Ishizuka Y, Ueda K, Okada H, Takeda J, Karashima M, Yazawa K, *et al.* Effect of drug-polymer interactions through hypromellose acetate succinate substituents on the physical stability on solid dispersions studied by fourier-transform infrared and solid-state nuclear magnetic resonance. Mol Pharm. 2019; 16(6): 2785–94.
12. Que C, Qi Q, Zemlyanov DY, Mo H, Deac A, Zeller M, *et al.* Evidence for halogen bonding in amorphous solid dispersions. Cryst Growth Des. 2020; 20(5): 3224–35.
13. Atsukawa K, Amari S, Takiyama H. Solid dispersion melt crystallization (SDMC) concept using binary eutectic system for improvement of dissolution rate. J Ind Eng Chem. 2021; 101: 21–7.
14. Alatas F, Ratih H, Sutarna TH, Fauzi ML. The binary and ternary amorphous systems of candesartan cilexetil preparation to improve its solubility. Int J Appl Pharm. 2024; 16(5): 367–72.
15. Borde S, Paul SK, Chauhan H. Ternary solid dispersions: Classification and formulation considerations. Drug Dev Ind Pharm. 2021; 47(7): 1011–28.
16. Sohn JS, Kim EJ, Park JW, Choi JS. Piroxicam ternary solid dispersion system for improvement of dissolution (%) and in vitro anti-inflammation effects. Mater Sci Eng B. 2020; 261: 114651. doi: 10.1016/j.mseb.2020.114651.
17. Saberi A, Kouhjani M, Yari D, Al. E. Development, recent advances, and updates in binary, ternary co-amorphous systems, and ternary solid dispersions. J Drug Deliv Sci Technol. 2023; 86: 104746. doi: 10.1016/j.jddst.2023.104746.
18. Budiman A, Lailasari E, Nurani NV, Yunita EN, Anastasya G, Aulia RN, *et al.* Ternary solid dispersions: A review of the preparation, characterization, mechanism of drug release, and physical stability. Pharmaceutics. 2023; 15(8): 2116. doi: 10.3390/pharmaceutics15082116.
19. Amaliah S, Aulifa D, Gazzali A, Budiman A. Ternary solid dispersions as an alternative approach to enhance pharmacological activity. Drug Des Devel Ther. 2025; 19: 5663–84.
20. Budiman A, Citraloka ZG, Muchtaridi M, Sriwidodo S. Inhibition of crystal nucleation and growth in aqueous drug solutions: Impact of different polymers on the supersaturation profiles of amorphous drugs — The case of alpha-mangostin. Pharmaceutics. 2022; 14(2386): 2386. doi: 10.3390/pharmaceutics14112386.
21. Park CW, Tung NT, Rhee YS, Kim JY, Oh TO, Ha JM, *et al.* Physicochemical, pharmacokinetic and pharmacodynamic evaluations of novel ternary solid dispersion of rebamipide with poloxamer 407. Drug Dev Ind Pharm. 2013; 39(6): 836–44.
22. Munir R, Hadi A, Khan SUD, Asghar S, Irfan M, Khan IU, *et al.* Solubility and dissolution enhancement of dexibuprofen with hydroxypropylbetacyclodextrin (HPβCD) and poloxamers (188/407) inclusion complexes: Preparation and in vitro characterization. Polymers. 2022; 14(3): 579. doi: 10.3390/polym14030579.
23. Greenspan L. Humidity Fixed Points of Binary Saturated Aqueous Solutions. J Res Natl Bur Stand A Phys Chem. 1977; 81A(1): 89–96.
24. Baird JA, Van Eerdenbrugh B, Taylor LS. A classification system to assess the crystallization tendency of organic molecules from undercooled melts. J Pharm Sci. 2010; 99(9): 3787–806.
25. Budiman A, Aulifa DL. A comparative study of the pharmaceutical properties between amorphous drugs loaded-mesoporous silica and pure amorphous drugs prepared by solvent evaporation. Pharmaceuticals. 2022; 15(6): 730. doi: 10.3390/ph15060730.
26. Budiman A, Nurani NV, Laelasari E, Muchtaridi M, Sriwidodo S, Aulifa DL. Effect of drug–polymer interaction in amorphous solid dispersion on the physical stability and dissolution of drugs: The case of alpha-mangostin. Polymers. 2023; 15(14): 3034. doi: 10.3390/polym15143034.
27. Salamah R, Wijayanti N, Widiyanto S. n-hexane fraction of Cucumis melo L. cultivar gama melon parfum: An in vitro study in MCF7 and T47D cells line. Mol Cell Biomed Sci. 2025; 9(2): 76–81.
28. Budiman A, Handini AL, Muslimah MN, Nurani NV, Laelasari E, Kurniawansyah IS, *et al.* Amorphous solid dispersion as drug delivery vehicles in cancer. Polymers. 2023; 15(16): 3380. doi: 10.3390/polym15163380.
29. Shah N, Iyer RM, Mair HJ, Choi DS, Tian H, Diodone R, *et al.* Improved human bioavailability of vemurafenib, a practically insoluble drug, using an amorphous polymer-stabilized solid dispersion prepared by a solvent-controlled coprecipitation process. J Pharm Sci. 2013; 102(3): 967–81.
30. Rizal MI, Sandra F. Brucea javanica leaf rxtract activates caspase-9 and caspase-3 of mitochondrial apoptotic pathway in human oral squamous cell carcinoma. Indones Biomed J. 2016; 8(1): 43–8.
31. Alkathiri FA, Bukhari SI, Imam SS, Alshehri S, Mahdi WA. Formulation of silymarin binary and ternary solid dispersions: Characterization, simulation study and cell viability assessment against lung cancer cell line. Heliyon. 2024; 10(1): e23221. doi: 10.1016/j.heliyon.2023.e23221.
32. Widowati W, Jasaputra DK, Sumitro SB, Widodo MA, Afifah E, Rizal R, *et al.* Direct and indirect effect of TNFα and IFNγ toward apoptosis in breast cancer cells. Mol Cell Biomed Sci. 2018; 2(2): 60–9.
33. Haq SA, Paudwal G, Banjare N, Iqbal Andrabi N, Wazir P, Nandi U, *et al.* Sustained release polymer and surfactant based solid dispersion of andrographolide exhibited improved solubility, dissolution, pharmacokinetics, and pharmacological activity. Int J Pharm. 2024; 651: 123786. doi: 10.1016/j.ijpharm.2024.123786.
34. Mane PT, Wakure BS, Wakte PS. Ternary inclusion complex of docetaxel using β-cyclodextrin and hydrophilic polymer: Physicochemical characterization and in-vitro anticancer activity. J Appl Pharm Sci. 2022; 12(12): 150–61.
35. Copetti PM, Bissacotti BF, da Silva Gündel S, Bottari NB, Sagrillo

MR, Machado AK, *et al.* Pharmacokinetic profiles, cytotoxicity, and redox metabolism of free and nanoencapsulated curcumin. J Drug Deliv Sci Technol. 2022; 72: 103352. doi: 10.1016/j.jddst.2022.103352.

36. Chung CK, Fransen MF, van der Maaden K, Campos Y, García-Couce J, Kralisch D, *et al*. Thermosensitive hydrogels as sustained drug delivery system for CTLA-4 checkpoint blocking antibodies. J Control Release. 2020: 323: 1–11. doi: 10.1016/j.jconrel.2020.03.050.
37. Iyer R, Jovanovska VP, Berginc K, Jaklic M, Fabiani F, Harlacher C, *et al.* Amorphous solid dispersions (ASDs): the influence of material properties, manufacturing processes and analytical technologies in drug product development. Pharmaceutics. 2021; 13(10): 1682. 1682. doi: 10.3390/pharmaceutics13101682.
38. Holm TP, Kokott M, Knopp MM, Boyd BJ, Berthelsen R, Quodbach J, *et al.* Development of a multiparticulate drug delivery system for in situ amorphisation. Eur J Pharm Biopharm. 2022; 180: 170–80.